processes

MDPI

Article

Estimating the Influencing Factors of Gas–Water Relative Permeability in Condensate Gas Reservoirs under High-Temperature and High-Pressure Conditions

Shuheng Cui [1,*], Qilin Wu [2,*] and Zixuan Wang [2]

[1] CNOOC Energy Technology & Services Limited, CNOOC EnerTech Drilling & Production Zhanjiang Branch, Zhanjiang 524057, China
[2] College of Petroleum Engineering, Guangdong University of Petrochemical Technology, Maoming 525000, China; wzx19120863171@163.com
* Correspondence: cuishh@cnooc.com.cn (S.C.); wuqilin9@gdupt.edu.cn (Q.W.)

Abstract: The gas–water relative permeability curve plays a crucial role in reservoir simulation and development for condensate gas reservoirs. This paper conducted a series of high-temperature and high-pressure analysis experiments on real gas cores from Wells A and B in Block L of the Yinggehai Basin to investigate the effects of temperature, pressure, and different types of gas media on gas–water seepage. The gas–water relative permeability was simulated in this experiment through variations in temperature, pressure, and gas composition. Temperature has a significant impact on both gas and water relative permeability, particularly on gas relative permeability. As temperature increases, gas relative permeability shows a substantial increase, while water relative permeability remains relatively unchanged. Under the same effective stress, increasing pressure causes downward shifts in both the gas and water relative permeability curves; however, there is a more pronounced decrease in gas relative permeability. Gas composition has minimal influence on the gas–water relative permeability except at higher water saturation where differences become apparent. When water saturation ranges from 80% to 50%, there is no significant variation observed in the measured relative permeability of different displacement gases. However, as water saturation exceeds 80%, distinctions gradually emerge. The relative permeability of nitrogen is approximately 92% lower than that of mixed gas when the bound water saturation reaches 80%. This investigation provides valuable insights into the characteristics of gas–water relative permeability in high-temperature and high-pressure condensate reservoirs within Yinggehai Basin, thereby offering significant contributions to development strategies for similar reservoirs.

Keywords: gas–water relative permeability; high temperature; high pressure; condensate gas reservoir; influencing factors

Citation: Cui, S.; Wu, Q.; Wang, Z. Estimating the Influencing Factors of Gas–Water Relative Permeability in Condensate Gas Reservoirs under High-Temperature and High-Pressure Conditions. *Processes* **2024**, *12*, 728. https://doi.org/10.3390/pr12040728

Academic Editor: Brice Bouyssiere

Received: 2 March 2024
Revised: 27 March 2024
Accepted: 29 March 2024
Published: 3 April 2024

1. Introduction

Natural gas is a naturally gaseous hydrocarbon mixture that is formed under the earth's surface [1]. Natural gas is considered to be the cleanest fossil fuel and is a safe source of energy when transported, stored, and used. The Yinggehai Basin in the South China Sea harbors abundant natural gas resources characterized by high-temperature and -pressure conditions, with temperatures reaching up to 216 °C and pressures peaking at 13,485 psi. However, the extreme temperature and pressure systems pose challenges for the development of such reservoirs. Not only do they impose more rigorous technical requirements throughout the development process, but they also pave the way for novel avenues of research into fluid physical properties. For instance, high-temperature and high-pressure formation fluids exhibit large deviation coefficients ($Z > 2.0$), surpassing typical industry charts ($Z \leq 1.7$) commonly used for the evaluation of gas reservoir reserves and

engineering calculations [2]. Moreover, the fluids often display near-critical characteristics due to condensate gas properties, such as low gas–liquid surface tension [3].

The measurement methods, experimental procedures, and analyses of experimental results of gas–water relative permeability have been extensively researched by both domestic and international scholars [4]. The Buckley–Leverett displacement mechanism is effectively applied in waterflooding performance [5]. Rapoport and Leas introduced the concept of an unsteady relative permeability testing method, followed by further investigations carried out by Potter [6]. Furthermore, the study examines the gas-water flow behavior in fractures, with a particular focus on how water saturation affects the relative permeability coefficient of the gas phase. The findings indicate that an increase in water saturation leads to a decrease in gas relative permeability [7]. The gas–water relative permeability of coal cores was assessed using the unsteady state method to measure and establish the phase permeability curve [8]. A method measured fractal flow experimental data related to gas relative permeability and water relative permeability during gas–water two-phase seepage [9]. Although the experimental principle for obtaining gas–water relative permeability is relatively clear, there is still a lack of research on high-temperature (>100 °C) and high-pressure (>5801 psi) conditions, resulting in an unclear understanding of the relative permeability law.

In light of the current limitations in experimental instruments for measuring gas–water relative permeability under high-temperature and high-pressure conditions, this paper presents a set of precise gas–water phase permeability measurement equipment capable of accurately separating and quantifying water and gas output at temperatures up to 250 °C and pressures up to 18,130 psi. The gas–water relative permeability of three cores from Wells A and B in Yinggehai Basin is examined under these extreme formation conditions, elucidating the effects of varying temperatures, pressures, and gas compositions on the characteristics of gas–water phase infiltration.

2. Materials and Methods

2.1. Experiment

It is challenging to attain the required temperature and pressure during the execution of high-temperature and high-pressure gas–water relative permeability experiments using traditional experimental devices. The precision of water quantity measurements and the fluctuation in the back-pressure valve also significantly impact test results. In high-temperature and high-pressure gas reservoirs, the rock's pore volume undergoes compression due to elevated pressure, resulting in a reduction in porosity. It is noteworthy that the presence of water at the core's end leads to a significant decline in gas production within a short period, accompanied by a rapid increase in water content. Consequently, conventional measurement methods fail to achieve precise measurements.

Therefore, an independently designed relative permeability measurement device has been developed that enables accurate separation and quantification of effluent and gas volumes under high-temperature and high-pressure conditions.

The device comprises a high-temperature and high-pressure core gripper, thermostat, electric displacement pump, back-pressure pump, gas–water separation metering device, gas booster pump, and console. The high-temperature and high-pressure core holder can withstand temperatures up to 250 °C and pressures up to 17,404 psi. The thermostat can be heated stably up to 280 °C.

The gas–water separation metering device enables the full and rapid separation of gas and water while achieving real-time measurements with the visualization capillary method and image recognition-based gas–liquid interface method with an accuracy of up to 0.05 mL, which meets the requirements for high-temperature and -pressure experiments. Figure 1 illustrates the experimental flow for measuring gas–water relative permeability under high-temperature and -pressure conditions.

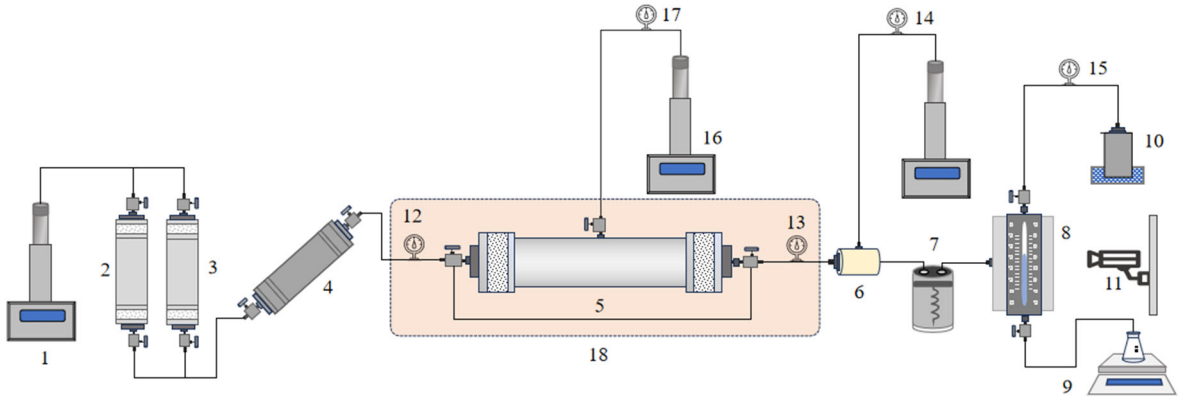

Figure 1. Experimental process of gas–water relative permeability under high-temperature and high-pressure conditions. 1. Displacement pump; 2. Gas intermediate container; 3. Water intermediate container; 4. Air–water balance shaker; 5. Gripper; 6. Pressure valve; 7. Cooling device; 8. Gas–liquid separator; 9. Balance; 10. Gas meter; 11. Industrial cameras; 12. Inlet pressure gauge; 13. Export pressure gauge; 14. Back-pressure gauge; 15. Back-pressure pump; 16. Confining pressure pump; 17. Confining pressure gauge; 18. Thermostat.

The experimental measurement device for gas–water relative permeability under high-temperature and high-pressure conditions in the laboratory is depicted in Figure 2. The figure includes labels indicating the names of significant equipment.

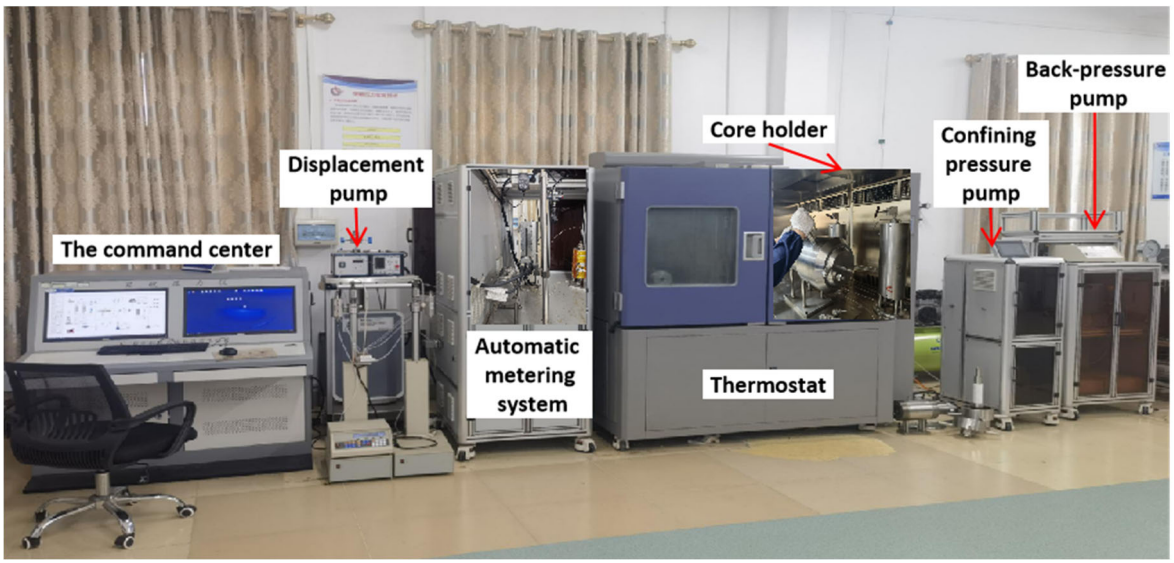

Figure 2. The experimental device for measuring gas–water relative permeability under high temperature and high pressure and the crucial pieces of equipment, including the command center, displacement pump, automatic metering system, thermostat, core holder, confining pressure pump and back-pressure pump.

2.2. Samples

(1) Core

The cores used in the experiment were real cores taken from the target interval of the gas reservoir of Well A and Well B. Cores with relatively little damage were selected for numbering and trimming. Their basic parameters are shown in Table 1. The core permeability of the Well A gas reservoir is about 6 μD, and that of the Well B gas reservoir is about 2.5 μD, both of which are low-permeability cores.

Table 1. Physical parameters of the core samples.

Core Number	Length (cm)	Diameter (cm)	Weight (g)	Pressure (psi)	Porosity (%)	Permeability (mD)
Well A 1-14	3.478	2.502	37.3767	493	19.32	6.1480
Well B 2-12	3.294	2.476	35.0675	493	16.73	2.5540
Well B 2-20	3.438	2.474	36.1635	493	17.98	2.4300

(2) Mixed Gas

The natural gas composition of the Well B reservoir is mainly methane, the molar content is 88.6%, and the composition also contains a small amount of CO_2 and N_2. According to this composition, a mixed gas was configured to carry out core displacement experiments.

(3) Formation Water

The original data showed that the formation water salinity was 36,491 mg/L.

2.3. Experimental Plan

The present experiment is based on the gas–water relative permeability test conducted under conditions of high temperature and high pressure. Three different experimental conditions, including varying temperatures, pressures, and gas compositions, were selected to measure the relative permeability results. Based on these experimental findings, the impacts of temperature, pressure, and gas composition on the infiltration behavior of gas–water two phase flow under high temperature and high pressure were discussed.

For the confirmed core and formation water, the main factors affecting gas–water relative permeability are pressure, temperature, and gas composition. Aiming at these influencing factors, a series of experiments were designed, and the experimental scheme is shown in Table 2.

Table 2. Parameters of the core samples.

Sample #	Core No.	Permeability (mD)	Influencing Factors
1	Well A 1-14	6.1480	stress
2	Well B 2-12	2.5540	temperature
3	Well B 2-20	2.4300	temperature
4	Well B 2-12	2.5540	gaseous medium

2.4. Core Saturation

The gas test method was employed to measure the permeability (Kg) and porosity (Φ) of each core. The core, with a length (L) and diameter (D), should be dried at a temperature of 116 °C for a minimum duration of 4 h. Subsequently, the dried core is to be removed and cooled in a dryer. Once cooled, the weight (m1) after drying is determined using an electronic balance.

After weighing, the core and saturated water are subjected to vacuuming at a pressure of 1.3 Pa for a minimum of 4 h each. Following this, the rock ventricle is injected with saturated water and vacuumed for an additional hour. Once the saturated water has been pumped out, the vacuum device is closed and the valve connected to the atmosphere of the rock chamber is opened, allowing it to rest for 12 h.

The experimenter removed the saturated core and dried the surface of the floating water. The weight, m2, after core saturation was measured experimentally, and the porosity, Φ_1, was calculated based on core liquid measurements. If the relative error between porosity Φ_1 and porosity Φ is less than 2%, saturation is considered complete. Otherwise, pressure saturation will be conducted by applying a pressure of 725 psi to 2901 psi without causing any damage to the core. After saturating for more than 12 h, the recalculated core fluid porosity Φ_1 was determined.

2.5. The Formation Temperature and Pressure Conditions

The experimenter placed the core into the core holder, introduced formation water into the intermediate container, and pressurized the experimental gas for utilization. After connecting the experimental process, the return pressure valve was initially pressurized to 725 psi, followed by the driving of the core using formation water until water flowed out from the outlet. Upon reaching the outlet end of water flow, the back pressure was increased by 290 psi while maintaining a displacement pressure of 290 psi. To prevent damage to the core, this increase in back pressure simultaneously raised both the confining and displacement pressures while maintaining a stress difference between them at approximately 725 psi to 1160 psi.

Once the internal pressure reached the formation pressure, further incrementation ceased and only the confining pressure above the overlying formation pressure was increased. The incubator was utilized to heat up to the formation temperature.

Through these aforementioned experimental procedures, personnel successfully established the conditions of formation temperature and pressure.

2.6. Water-Phase Permeability

The water phase permeability, serving as the fundamental parameter for water–gas relative permeability, is determined through constant pressure displacement experiments. Once the experiment reaches a stable state in terms of pressure and flow rate, the inlet pressure, outlet pressure, and flow rate are recorded. The Darcy Formula (1) is then employed to calculate the water permeability.

To meet experimental requirements, three consecutive measurements of the water phase permeability are conducted with a relative deviation of less than 3%. This ensures the accurate determination of the water phase permeability.

$$K = \frac{Q\mu_w L}{A\Delta P} \times 100 \quad (1)$$

where K is the water phase permeability under formation conditions, mD; Q is the flow rate through the core under formation conditions, mL/s; μ_w is the viscosity of water under formation conditions, mPa·s; L is the core length, cm; A is the core cross-sectional area, cm^2; and ΔP is the pressure difference between the inlet and outlet of the core, MPa.

2.7. Gas Drive

To determine the relative permeability curve of high-temperature and high-pressure solution gas drive using the constant pressure method. It is crucial to carefully select an appropriate displacement pressure difference. The chosen pressure difference must ensure that turbulence does not occur during the experiment.

Maintain a constant pressure in the displacement pump based on the selected displacement pressure difference. Once the pressure stabilizes, initiate data collection by clicking on the software. The software will automatically record parameters such as liquid production, gas production, inlet pressure, outlet pressure, and time. The data collection interval should be set between 2 to 10 s. Subsequently, commence the solution gas drive experiment.

After completion of the experiment, measure the effective permeability of the gas at both half- and quarter-displacement pressures, respectively. Based on the disparity between the low-pressure and high-pressure permeabilities, determine if turbulent flow has occurred. Typically, if the low-pressure differential permeability exceeds 10% of its high-pressure counterpart, it indicates turbulence in this experiment.

2.8. Water Drive

After conducting the gas-driven water experiment, gradually increase the displacement pressure differential until no further water efflux is observed, and meticulously document the cumulative water production. The aforementioned recorded total water production will be converted to reflect formation conditions, enabling computation of the

irreducible water saturation, Sw, based on the correlation between the irreducible water saturation under formation conditions and the total pore volume of the core.

The determination of confined underwater gas permeability is conducted by setting the displacement pressure and stabilizing the pressure and flow rate. Subsequently, the inlet pressure, outlet pressure, and flow rate are recorded to calculate the gas phase permeability using Formula (2). To complete the measurement of the gas phase permeability, three consecutive measurements are performed with a relative deviation of less than 3%. This measured gas permeability serves as the fundamental value for the water-driven gas relative permeability.

$$K = \frac{2P_2 Q \mu_g L}{A\left(P_1^2 - P_2^2\right)} \times 100 \quad (2)$$

K is the gas phase permeability under formation conditions, mD. Q is the flow rate through the core under formation conditions, mL/s. μ_g is the viscosity of gas under formation conditions, mPa·s. L is the core length, cm. A is the core cross-sectional area, cm^2. P_2 is the pressure at the outlet end of the core under the formation condition, MPa. P_1 is the pressure at the inlet of the core under the formation condition, MPa.

The water-driven gas flow proceeds as follows: based on selected displacement pressure difference or flow rate, set up a displacement pump and initiate data collection. Record liquid production, gas production, inlet pressure, outlet pressure, and time while setting interval between 2 and 10 s. Commence with the water–gas displacement experiment.

3. Correction

The measurement of the gas–water relative permeability curve under room conditions follows the Buckley–Leverett equation. Under the environment of high pressure high temperature, the dissolved gas amount will have a large increase in the formation water, and the volume of water and gas will have a large change too. Thus, the cumulative water (V_w) and cumulative gas (V_g,) will have a large difference between the room environment and the formation environment. As a result, we should make correction for the parameters from room to formation by using the following equations [10].

3.1. Water Volume

The water volume correction, accounting for the variation volume from underground formation conditions to the surface, is performed using Formula (3).

$$V_w = V_{sw} \times B_w \quad (3)$$

The water volume V_w (mL) under formation conditions is determined by the product of the liquid volume Vsw (mL) and the surface condition's volume factors of water B_w.

3.2. Gas Volume

The gas volume correction, accounting for the variation in gas volume from underground formation conditions to the surface, is performed using Formula (4).

$$V_g = V_{sg} \times B_g \quad (4)$$

The volume of gas V_g (mL) under formation conditions is determined by multiplying the gas volume V_{sg} (mL) under ground conditions with the volume factors of gas B_g.

3.3. Average Pressure Correction of Gas Volume

The average pressure correction of the gas volume is shown in Formula (5).

$$V_i = \Delta V_{0(w)i} + V_{i-1} + \frac{2P_2}{\Delta P + 2P_2} \Delta V_{gi} \quad (5)$$

where V_i is the value of the cumulative moisture production at time i, mL; $\Delta V_{0(w)i}$ is the value of the water increment from time $i-1$ to time i, mL; V_{i-1} is the value of the accumulated moisture production at the time $i-1$, mL; P_2 is the pressure at the outlet end of the core under the formation condition, MPa; ΔP is the displacement pressure difference, MPa; and ΔV_{gi} is the value of the gas increment measured at the outlet at a certain time interval, mL.

3.4. Gas–Water Relative Permeability Calculation Method

The unsteady gas–water relative permeability characterization method was developed based on the calculation formula for oil–water phase permeability.

For the calculation method of the gas drive, refer to Formulas (6)–(10).

$$fw(Sg) = \frac{dV_w(t)}{dV(t)} \tag{6}$$

$$Krw = fw(Sg)\frac{d(1/V(t))}{d(1/IV(t))} \tag{7}$$

$$Krg = Krw\frac{\mu_g}{\mu_w}\frac{1-fw(Sg)}{fw(Sg)} \tag{8}$$

$$Sg = V_w(t) - V(t)fw(Sg) \tag{9}$$

$$I = \frac{Q(t)}{Q_0}\frac{\Delta P_0}{\Delta P(t)} \tag{10}$$

where $fw(Sg)$ is the value of water content, expressed as a decimal; $V_w(t)$ is the value of dimensionless cumulative water recovery, expressed as a multiple of pore volume; $V(t)$ is the value of dimensionless cumulative production, expressed as a multiple of the pore volume; Krw is the value of the relative permeability of the water phase, expressed as a decimal; Krg is the gas phase relative permeability value, expressed as a decimal; I is the value of the relative injection capacity, also known as flow capacity; and Sg is the value of gas saturation on the end face of the outlet of the rock sample, expressed as a decimal.

The water driven calculation is shown in Formulas (11)–(14). In addition, the value of the relative injection capacity is calculated by reference to Formula (10).

$$fg(Sw) = \frac{dV_g(t)}{dV(t)} \tag{11}$$

$$Krg = fg(Sw)\frac{d(1/V(t))}{d(1/IV(t))} \tag{12}$$

$$Krw = Krg\frac{\mu_w}{\mu_g}\frac{1-fg(Sw)}{fg(Sw)} \tag{13}$$

$$Sw = Sws + Vg(t) - V(t)fg(Sw) \tag{14}$$

where $fg(Sw)$ is the value of the gas content, expressed as a decimal; $Vg(t)$ is the value of the cumulative amount of water extracted without a result, expressed as a multiple of the pore volume; $V(t)$ is the value of cumulative production without a result, expressed as a multiple of pore volume; Krw is the value of the relative permeability of the water phase, expressed as a decimal; Krg is a numerical value of the relative permeability of the gas phase, expressed as a decimal; I is the value of the relative injection capacity, also known as flow capacity; and Sw is the value of the water saturation of the outlet end face of the rock sample, expressed as a decimal.

4. Results

The majority of domestic and foreign experiments on the gas–water relative permeability at high temperature and high pressure are limited to either high-temperature or high-pressure conditions.

Furthermore, even the research conducted under high temperature and high pressure falls significantly below the current formation pressure of high-pressure gas reservoirs. Additionally, there is a lack of quantitative comparison between conventional and high-temperature/high-pressure relative permeability using the same core [11,12].

4.1. Effect of Temperature on Gas–Water Relative Permeability

The gas–water relative permeability experiment was conducted on core 2–12 of Well B at temperatures of 180 °C and 100 °C, while core 2–20 of Well B was selected for the experiment at temperatures of 160 °C and 130 °C. Mixed gas was used as the medium, and the experimental pressure was maintained at 70 MPa. The resulting gas–water relative permeability curve is presented in Figure 3. The experimental findings demonstrate that temperature exerts a significant influence on both gas and water relative permeability, particularly on the former.

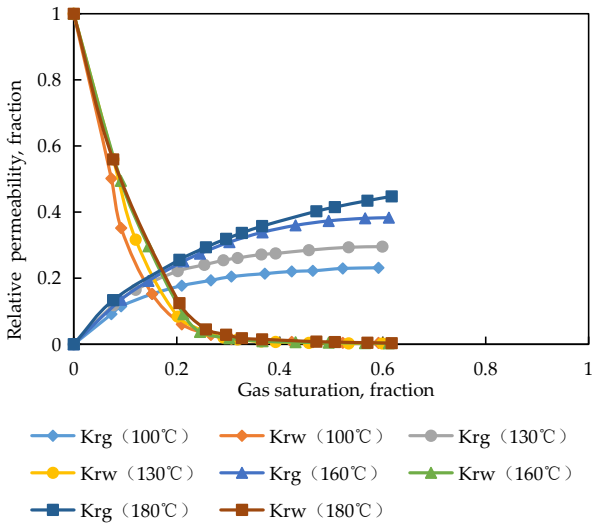

Figure 3. Measurement results of the gas–water relative permeability at different temperature conditions.

With the rise in temperature, the saturation of the bound water decreases, leading to an expansion of the gas–water two-phase seepage zone. Additionally, there is a significant increase in relative permeability for the gas phase, while minimal changes occur for the water phase. Consequently, the gas–water relative permeability curve shifts towards the upper left.

This phenomenon can be attributed to the larger intermolecular spacing within gas molecules, making them more sensitive to temperature and exhibiting increased activity as temperature rises. As a result, their relative permeability increases accordingly. Elevated temperatures also enhance molecular motion, facilitate gas dissolution, and reduce interfacial tension between the gas and water phases. The effects collectively diminish water phase entrapment within pores and adhesion on rock surfaces, ultimately resulting in a decrease in irreducible water saturation with increasing temperature. Furthermore, higher temperatures lead to a gradual convergence of gas–water viscosities along with decreased interfacial tension and capillary pressure, consequently widening the gas–water two-phase seepage zone and gradually improving overall sweep efficiency.

4.2. Effect of Pressure on Gas–Water Relative Permeability

The experimental sample chosen for analysis was Core 1–14 of Well A in Block A. Utilizing mixed gas as the medium, the determination of the gas–water relative permeability was conducted using the constant pressure method at an experimental temperature of 160 °C and varying experimental pressures of 10,153 psi, 7521 psi, 4351 psi, and 1450 psi respectively.

The gas–water relative permeability curves under different fluid pressures are depicted in Figure 4. It is evident from the curve that, at a constant effective stress, both the gas and water phases exhibit a downward shift in their respective relative permeability curves with increasing experimental fluid pressure. Notably, when the fluid pressure reaches 1450 psi and 4351 psi, the gas relative permeability curves display similar trends. Similarly, at fluid pressures of 7521 psi and 10,153 psi, there is close resemblance between the gas relative permeability curves.

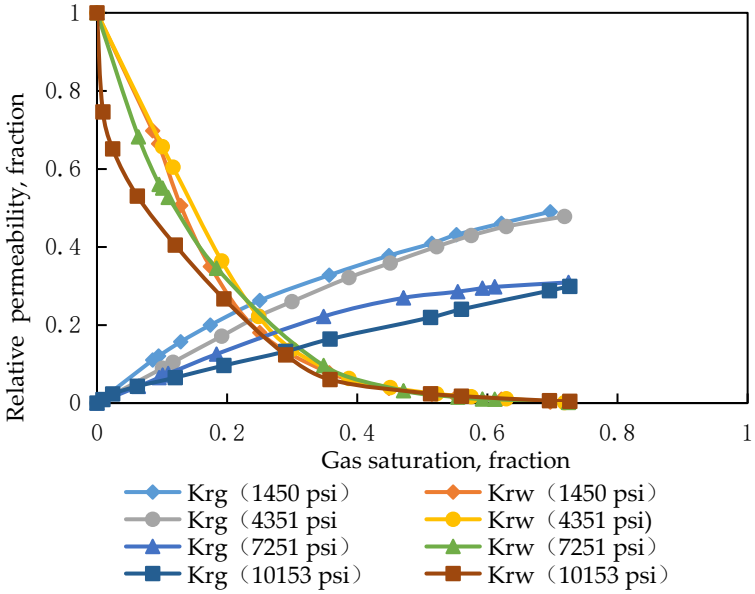

Figure 4. Measurement results of the gas–water relative permeability under different pressure conditions.

This is closely related to temperature–pressure and core physical property parameters during the experiment. With the increase in experimental fluid pressure, the viscosity of the gas and formation water increases, but the increase proportions are different, resulting in different gas–water relative permeability changes.

The experimental results demonstrate that the pressure drop during formation significantly impacts the gas–water relative permeability curve. Under a specific confining pressure, as the experimental fluid pressure decreases, the effective stress on the core increases, leading to a decrease in both the gas relative permeability and the water relative permeability. Additionally, there is an increase in irreducible water saturation, expansion of the gas–water two-phase infiltration zone, and a shift of the isosmotic point towards higher water saturation.

4.3. Influence of Different Gas Composition

The experiment aimed to investigate the impact of different displacement gases on the gas–water relative permeability of. For this purpose, core 2–12 from Well B in block A was selected as the sample. Mixed gas and nitrogen were employed as the media during the experiment. The gas–water relative permeability curves were measured under conditions of 180 °C and 70 MPa.

The gas–water relative permeability curves under different displacement gas compositions are depicted in Figure 5. It can be observed from the figure that the gas composition exerts minimal influence on the gas–water relative permeability curve. Overall, there is no significant variation in the relative permeability of gas to water measured by different displacement gases when the water saturation ranges between 80% and 50%.

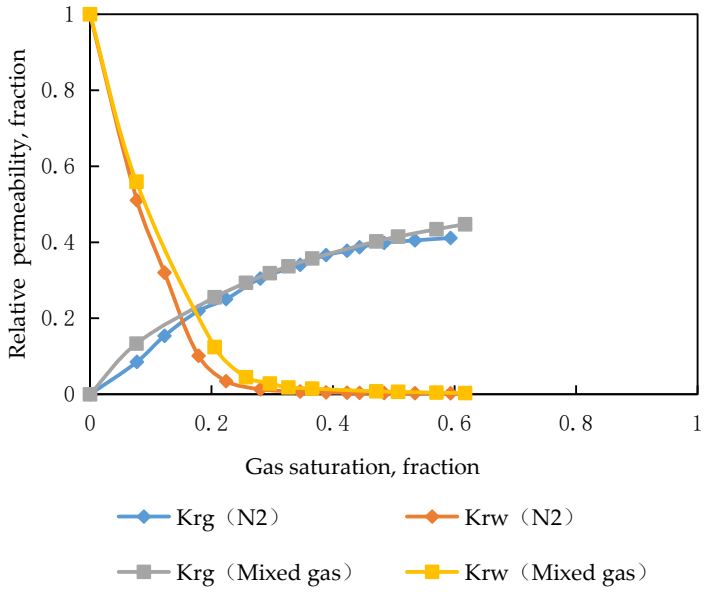

Figure 5. Measurement results of the gas–water relative permeability of different gas compositions.

When the water saturation exceeds 80%, the disparity in the gas–water relative permeability curves becomes progressively evident. Under conditions of irreducible water saturation, the nitrogen-based gas–water relative permeability is approximately 92% of the mixed gas equivalent, indicating a higher solubility of mixed gas compared to nitrogen under high temperature and pressure.

Consequently, the measured method yields a greater gas–water relative permeability than that observed with nitrogen.

5. Conclusions

1. This study describes the independent development of a relative permeability measuring device capable of operating under high-temperature and high-pressure conditions, enabling accurate separation and measurement of water and gas.
2. The experimental device has a maximum temperature capability of 250 °C and can withstand pressures up to 18,130 psi, facilitating efficient and rapid gas–water separation with a measurement accuracy as fine as 0.05 L.
3. The experimental results show that the temperature has a certain effect on the gas–water relative permeability. With a rise in temperature, the saturation of bound water decreases, leading to an expansion of the gas–water two-phase seepage zone. Additionally, there is a significant increase in relative permeability for the gas phase, while minimal changes occur for the water phase.
4. The experimental results demonstrate that the pressure drop during formation significantly impacts the gas–water relative permeability curve. Under a specific confining pressure, as the experimental fluid pressure decreases, the effective stress on the core increases, leading to a decrease in both the gas relative permeability and the water relative permeability. Additionally, there is an increase in the irreducible water saturation, expansion of the gas–water two-phase infiltration zone, and a shift of the isosmotic point towards higher water saturation.

5. The gas composition has little influence on the phase permeability, and the main influence is shown at high water saturation. Changes in the relative permeability of the gas phase as measured by different displacement gases are not obvious when the water saturation is 80–50%. When the water saturation is higher than 80%, the difference is gradually obvious. Under the condition of irreducible water saturation, the relative permeability of nitrogen is less than that of mixed gas, about 92% of the latter.

Author Contributions: Methodology, S.C. and Q.W.; Data curation, Z.W. All authors have read and agreed to the published version of the manuscript.

Funding: This research was funded by the Innovation Project of Educational Commission of Guangdong Province grant number 2020KTSCX084.

Data Availability Statement: Data are contained within the article.

Conflicts of Interest: Author Shuheng Cui was employed by the company CNOOC Energy Technology& Services limited, CNOOC EnerTech Drilling& Production Zhanjiang Branch. The remaining authors declare that the research was conducted in the absence of any commercial or financial relationships that could be construed as a potential conflict of interest.

Nomenclature

A	core cross-sectional area, cm^2
Bg	volume factors of gas
Bw	volume factors of water
K	absolute permeability, mD
kr	relative permeability
krg	gas relative permeability
Krw	water relative permeability
μ_g	gas viscosity, MPa·s
μ_w	water viscosity, MPa·s
P_1	the pressure at the inlet of the core under the formation condition, MPa
P_2	the pressure at the outlet of the core under the formation condition, MPa
ΔP	the pressure differential between the core's inlet and outlet, MPa
I	the value of the relative injection capacity
L	core length, cm
Q	flow rate through the core under formation conditions, mL/s
Sg	gas saturation
S_w	water saturation
V_g	gas volume under formation conditions, mL
V_w	liquid volume under formation conditions, mL
Vsg	gas volume under ground conditions, mL
Vsw	liquid volume under ground conditions, mL

References

1. Faramawy, S.; Zaki, T.; Sakr, A.A.E. Natural gas origin, composition, and processing: A review. *J. Nat. Gas Sci. Eng.* **2016**, *34*, 34–54. [CrossRef]
2. Hao, G.; Yuan, S.; Song, W.; Li, H.; Luo, K. Fluid phase behavior and physical properties of Overpressured condensate gas reservoir. *J. Pet.* **2004**, *25*, 70–74.
3. Busahmin, B.; Maini, B.B. Measurements of surface tension for mineral and crude oil systems. In *Defect and Diffusion Forum*; Trans Tech Publications Ltd.: Bäch, Switzeralnd, 2019; Volume 391, pp. 106–113.
4. Shen, P. Review of methods for calculating relative permeability by displacement experiment. *Pet. Explor. Dev.* **1982**, *3*, 73–80.
5. Busahmin, B.; Karri, R.R.; Tyson, S.; Jami, M. Modeling of a long sand-pack for heavy crude oil through depletion tests utilizing methane ga. *Petroleum* **2021**, *7*, 188–198. [CrossRef]
6. Heaviside, J.; Brown, C.E.; Gamble, I.J.A. Relative Permeability for Intermediate Wettability Reservoirs. In Proceedings of the SPE Annual Technical Conference and Exhibition, Dallas, TX, USA, 27–30 September 1987; pp. 823–836.
7. Poilkar, M.; Farouq All, S.M.; Puttagunta, V.R. High-temperature relative permeability for Athabasca oil sands. *SPE Reserv. Eng.* **1990**, *5*, 25–32. [CrossRef]

8. Potter, G.; Lyle, G.L. Measuring Relative Permeability of High-Permeability Samples From Egypt. In Proceedings of the Society of Petroleum Engineers; Middle East Oil Show, Manama, Bahrain, 3–6 April 1993; pp. 53–62.
9. Mao, Q.; Fan, C.; Luo, J.; Cao, J.; You, L.; Fu, Y.; Li, S.; Shi, X.; Wu, S. Differential analysis of sedimentary diagenetic evolution of middle deep sandstone reservoirs under overpressure background: Takes Miocene Huangliu Formation in Yinggehai Basin, South China Sea as an example. *J. Paleogeogr.* **2022**, *24*, 344–360.
10. Yang, Z.; Li, Y.; Chen, Z.; Zhang, X.; Lu, K.; Du, X.; Guo, P. Measuring Gas-Water Relative Permeability in Tight Sandstones at High-Temperature High-Pressure Conditions: Experimental Design and Correction. In Proceedings of the SPE Reservoir Characterisation and Simulation Conference and Exhibition, Abu Dhabi, United Arab Emirates, 8–10 May 2017; p. D021S006R004.
11. Long, D.; Li, Y.; Shijiu, W.; Jia, Z.; Peiyuan, Z.; Zhanjie, Z. Physical property lower limit and classification of high-temperature and overpressure reservoirs in Ledong District, Yinggehai Basin. *Mar. Oil Gas Geol.* **2022**, *27*, 157–166.
12. Xiao, G.; Jingjing, M.; Jiudi, L.; Yang, H.; Haiying, W. Effect of reservoir temperature and pressure on relative permeability. In Proceedings of the SPETT 2012 Energy Conference and Exhibition, Port-of-Spain, Trinidad, 11–13 June 2012; paper number SPE 158055-MS.